Journal of Power Sources 253 (2014) 256–262

Contents lists available at ScienceDirect

Journal of Power Sources

journal homepage: www.elsevier.com/locate/jpowsour

Preparation and electrochemical performance of polyphosphazene based salt-in-polymer electrolyte membranes for lithium ion batteries

S. Jankowsky, M.M. Hiller, H.-D. Wiemhöfer*

Institute of Inorganic and Analytical Chemistry, University of Münster, Corrensstraße 28/30, 49149 Münster, Germany

HIGHLIGHTS

- Stable solvent-free polymer electrolyte membranes.
- Total ionic conductivity 0.16 mS cm^{-1} at 30 °C.
- Compatibility with metallic lithium electrodes, stable SEI, no degradation.
- Electrochemical stability window from 0 V up to 4.7 V vs. Li/Li^+.

ARTICLE INFO

Article history:
Received 21 August 2013
Received in revised form
23 October 2013
Accepted 28 November 2013
Available online 19 December 2013

Keywords:
Lithium ion batteries
Polymer electrolyte
Polyphosphazene
Ionic conductivity
Lithium transference number
Electrochemical stability

ABSTRACT

This work presents a detailed study of the electrochemical performance of polyphosphazene based electrolyte membranes consisting of a linear polymer with $-(N{=}PR_2)-$ units, grafted with ethylene oxide side chains of the type $R = -(OCH_2CH_2)_3OCH_3$ and containing LiTFSI and LiBOB as dissolved lithium salts. The average molecular weight was 10^5 g mol^{-1}. Mechanical stability was achieved by UV induced in-situ cross-linking of the thin polymer electrolyte films. Favorable properties of this type of polymer electrolytes are the good thermal and electrochemical stability of the electrolyte membranes, the broad electrochemical stability window ranging between 0 V and 4.7 V versus the Li/Li^+ reference and a very good interface stability at lithium metal electrodes where a stable SEI was formed during initial contact. Total ionic conductivities up to 10^{-4} S cm^{-1} were measured at 30 °C. The transference numbers of lithium ions at 50 °C ranged between 0.06 and 0.07 and hence are lower by a factor of about three as compared to other typical polymer electrolytes. Nevertheless, the partial lithium ion conductivity estimated from the product of total conductivity and lithium ion transference number is as high or slightly higher compared to PEO based polymer electrolytes.

1. Introduction

In recent years, the demand for more efficient and safer lithium ion batteries has increased, due to the growing interest in mobile devices and electric vehicles. Polymer gel electrolytes are already in use in lithium polymer batteries, e.g. based on poly(ethylene oxide) (PEO) or poly(vinylidene fluoride-co-hexafluoropropylene) (PVDF-HFP) swollen with liquid electrolytes like $LiPF_6$ containing EC/DMC mixtures [1,2]. The early investigations in the field of polymer electrolytes can be divided into solvent-free polymer electrolytes and gel polymer electrolytes (GPE). Since the first publications on salt solutions in PEO and their possible use as electrolytes [3–5], these and other solvent free polymer electrolytes have been considered as attractive candidates for battery applications, due to their safety, absence of volatility and less or negligible inflammability as compared to liquid electrolytes [2,6]. Mechanically stable cross-linked polymer electrolytes allow safe separation of anodes and cathodes, preventing short-circuits and dissolution of electrode components. Although solvent-free polymer electrolytes are often denoted as solid polymer electrolytes, the expression solid polymer is not correct as the corresponding polymers are used above their glass transition temperature and, thus correspond more to highly viscous fluids. In fact, as extensively reviewed [2,7], the ion transport is closely coupled to the segmental motion of the polymer molecules explaining also the observed non-Arrhenius temperature dependence of the conductivity which is well described by a Vogel–Fulcher–Tammann (VTF) equation in close analogy to the temperature dependence of the reciprocal viscosity of the polymer fluids.

As early as 1984, strongly improved ionic conductivities were demonstrated by choosing polyphosphazenes grafted with

* Corresponding author. Tel.: +49 251 83 33115; fax: +49 251 83 33193.
E-mail address: hdw@wwu.de (H.-D. Wiemhöfer).

0378-7753/$ – see front matter © 2013 Elsevier B.V. All rights reserved.
http://dx.doi.org/10.1016/j.jpowsour.2013.11.120

oligoethylene oxide side chains as solvents for lithium salts [8,9]. The advantage of oligoether grafted polyphosphazenes is their complete amorphous property together with an extremely low glass transition temperature which favors a high ionic mobility and solubility [10–14] and makes them attractive for a low temperature battery application. Recent experiences with good stability and performance of polyphosphazene based electrolytes in lithium ion cells as well as with lithium metal electrodes lead us to start more thorough investigations of their electrochemical behavior. The very good thermal and chemical stability of corresponding organo-modified polyphosphazenes and the availability of a convenient synthetic route towards high purity polymers by a living cationic polymerization were further arguments [15–17]. This work aims at the preparation and investigation of mechanically stable salt-in-polymer electrolyte membranes based on an oligoether grafted polyphosphazene with respect to electrochemical properties and stability versus lithium metal.

Furthermore, ion or mixed conducting inorganic polymers can be used as additives or binders in electrode structures by stabilizing the network of active particles and supporting the ion transport in such three-dimensional structures [18–20].

2. Experimental

2.1. Materials

All reactions were carried out under a dry nitrogen gas atmosphere using standard vacuum-line Schlenk techniques. Tetrahydrofurane (99.5%, *VWR*), *n*-pentane (98%, *Baker*) and toluene (99.7%, *VWR*) were freshly distilled from sodium benzophenone prior to use. Sulfuryl chloride (SO_2Cl_2 98%, *Aldrich*), phosphorous trichloride (PCl_3, 99%, *Merck KGaA*) and 2-(2-(2-Methoxyethoxy)ethoxy) ethanol ($C_7H_{16}O_4$, 99% *Merck KGaA*) were freshly distilled before use. Sodium hydride (NaH, 60% w/w dispersed in mineral oil, *Aldrich*), lithium bis(trimethylsilyl)amide ($LiN(Si(CH_3)_3)_2$, 97%, *Aldrich*) and phosphorous pentachloride (PCl_5, sublimated under vacuum) were stored under argon in a glove box. Lithium bis(trifluormethanesulfonyl)imide ($LiN(SO_2CF_3)_2$, purum, *Aldrich*) and lithium bis(oxalato)borate ($LiB(C_2O_4)_2$; 97%; *Chemetall GmbH*) were exclusively stored and handled in a dry room with water contents lower than 20 ppm and used as received. Chloroform-d (99.8 atom% D, *Aldrich*), lithium foil (*Chemetall GmbH*, 99.99%), platinum (*Chempur*, 99.99%, $Ø = 2$ mm) and nickel (*Alfa Aesar*, 99.98%) were used as received. Celite 545® (*Merck KGaA*) and the molecular sieve 4 Å (*VRW*) were dried at 140 °C for 48 h minimum before use. The dialysis tubes (*Reichelt Chemietechnik*, molecular weight cut off 12,000–14,000 g mol^{-1}) for polymer purification were washed and cleaned with distilled water before use.

2.2. Synthesis and membrane preparation

The synthesis of the monomer $Cl_3P{=}NSiMe_3$ was done in a dry Schlenk line under inert argon according to a synthetic route described by Wang et al. [16,21] with minor modifications [17]. Poly [dichlorophosphazene] (**4**) was synthesized from this monomer via living cationic polymerization using the route developed by Allcock et al. [22]. The final nucleophilic substitution of chlorine using the corresponding sodium alcoholate leads to the desired poly[bis 2-(2-(2-methoxyethoxy)ethoxy)ethoxyphosphazene] MEEEP (**5**) according to Scheme 1.

119.5 mmol of lithium bis(trimethylsilyl)amide (**1**) were dissolved in 300 mL of dry pentane. Freshly distilled phosphorous trichloride (114.6 mmol) was added drop wise within 30 min, while keeping the reaction temperature permanently at −15 °C. The reaction mixture was stirred for 30 min. Then sulfuryl chloride (106.1 mmol) was added drop wise under equal reaction conditions. After 30 min of stirring lithium chloride was precipitated, filtrated through Celite® and washed with 60 mL of dry *n*-pentane. After solvent evaporation the phosphoranimine monomer $Cl_3P{=}NSiMe_3$ (**2**) was vacuum distilled at 22 °C and 10^{-3} mbar. The monomer was received as a clear liquid with yields up to 70%. Afterward, phosphorous pentachloride was dissolved in dry toluene with concentration of about 11 mmol L^{-1}. The freshly prepared solution was added quickly to the monomer/toluene solution. The initiator-monomer ratio was 350:1. The polymerization product poly[dichloro-phosphazene] (**3**) was identified in the reaction mixture after 48 h by ^{31}P NMR. After solvent evaporation, the transparent, viscous precursor polymer (**3**) was received. ^{31}P NMR (400 MHz, $CDCl_3$, 300 K): δ (ppm) ∼ −17.97.

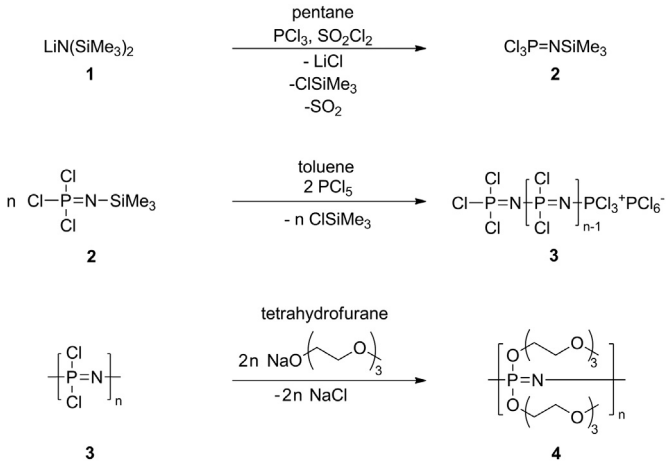

Scheme 1. The first two reactions describe the route to the precursor polymer (**3**) by the living cationic polymerization with PCl_5 as initiator; the third line describes the subsequent functionalization by nucleophilic substitution yielding MEEEP (**4**).

3.6 g (150 mmol) of sodium hydride was suspended in 120 mL tetrahydrofurane and cooled to 0 °C. The freshly distilled 2-(2-(2-methoxyethoxy)ethoxy)ethanol was added drop wise and the suspension was stirred for 1 h under hydrogen gas evolution. Then 8.7 g (74.9 mmol) of precursor polymer (**3**) dissolved in 50 mL tetrahydrofurane was added to the meanwhile clear solution and stirred for 24 h, while sodium chloride precipitated. Excess solvent was removed in a rotary evaporator. The product was purified in a dialysis tube (molecular weight cut off = 12.000–14.000 g mol^{-1}) against distilled water. After a final evaporation of water and drying at 50 °C under vacuum for 2 h, the highly viscous, yellow honey like poly[bis(2-(2-(2-methoxyethoxy)ethoxy)ethoxy phosphazene)] MEEEP (**4**) (M_w = 1.4979·10^5 g mol^{-1}, polydispersity index PDI = 1.32) was received in a yield of 24.7 g (66.5 mmol, 88%). ^1H NMR (400 MHz, $CDCl_3$, 300 K): δ (ppm) = 3.32 (3H, s), 3.58 (8H, m), 4.00 (2H, s), 3.49 (2H, m). ^{13}C NMR (101 MHz, $CDCl_3$, 300 K): δ (ppm) = 59.06 (s), 65.13 (s), 70.86–70.29 (m), 72.09 (s). ^{31}P NMR (400 MHz, $CDCl_3$, 300 K): δ (ppm) = −8.19 (s).

The salt-in-polymer electrolyte membranes were prepared by a solution casting technique as described in Ref. [23]. A solution of MEEEP (**4**) in tetrahydrofurane was mixed with different amounts of LiTFSI or LiBOB, as well as 5 wt% benzophenone. After stirring for 2 h the solvent was evaporated and then dried for at least 48 h at 70 °C under vacuum. Karl–Fischer titration revealed a remaining water content below 5 ppm. The homogeneous mixtures were sandwiched between two Mylar® foils and pressed to the thicknesses of ∼350 μm. Solid, flexible and transparent membranes were received after 10 min of UV-irradiation. Using 5 wt% benzophenone, a cross-linking degree of 10% was obtained as referred to

the monomer units (−NPR_2−). All samples were dried again after cross-linking for at least 48 h at 70 °C and, then, transferred into a glove box under dry argon.

2.3. Spectroscopic and thermal analysis

All NMR spectra were measured using a Bruker Avance III 400, Bruker Avance I 400 and a Bruker Avance II 200 spectrometer. $CDCl_3$ was used as solvent and trimethylsilane as internal standard. 85% H_3PO_4 was used as reference for the ^{31}P spectra.

The glass transition temperatures T_g of the polymers were obtained by DSC measurements in a temperature range between −150 °C and 150 °C. The DSC curves were recorded at a heating rate of 10 K min^{-1} under a dry nitrogen atmosphere using a Netzsch DSC 204.

2.4. Gel permeation chromatography

The molecular weights and molecular weight distributions (PDI) of the polymer MEEEP were analyzed by a gel permeation chromatograph from Polymer standards Service, Mainz, equipped with two PSS-SDV linear XL columns (8 mm × 300 mm, 5 μ), a RI detector (Agilent) and a viscosimeter detector (η-1001, WGE Dr. Bures). For the molecular weight estimation, a universal calibration curve was measured using polystyrene standards (Ready-Cal standard, Polymer Standards Service GmbH). Tetrahydrofurane with 0.1 wt% dissolved tetra-*n*-butylammonium bromide was used as solvent with a polymer concentration of 3.652 g L^{-1}. 50 μL of the sample solution were injected with a flow rate of 1 mL min^{-1}. With the weight average molecular weight divided by the number average molecular weight, the polydispersity index (PDI) is given by:

$$\mathrm{PDI} = \frac{\overline{M}_\mathrm{w}}{\overline{M}_\mathrm{n}} \tag{1}$$

All GPC data were analyzed with the software PSS WINGPC build 5403, which delivered the averaged molecular weight distributions $<M_W>$ and $<M_n>$ for the MEEEP polymer.

2.5. Cyclic voltammetry

Concerning the anodic and cathodic stability, the samples were studied via cyclic voltammetry (CV) in a three electrode cell versus a Li/Li^+ reference. The electrode potential corresponding to the oxidation stability limit were taken at a cut off current density of 0.05 mA cm^{-2} for beginning anodic decomposition, which is yet high enough to distinguish superimposed currents due to double layer charging and oxidation of minor impurities of the polymer electrolyte or the salt. All cells were thermo-stated (Phoenix II, *Haake*). Within ±0.1 K of the measuring temperature the CV curves were recorded, using a computer controlled potentiostat (Autolab PGSTAT302N, *Metrohm*) and carried out in a 3-electrode-cell, assembled under Argon atmosphere. Lithium foil was used for reference (RE: Ø = 5 mm) and counter electrodes (CE: Ø = 12 mm). The anodic oxidation limit was measured by cyclic voltammetry (scan rate 1 mV s^{-1}) in the range from 2.5 V to 6 V using an inert polarizable platinum working electrode. The cathodic reduction limit was determined analogously in the range 2.5 V to −0.5 V by choosing an inert nickel electrode as polarizable working electrode (as Pt would lead to lithium alloy formation for an electrode potential near zero). All working electrodes had a diameter of 1 mm. Prior to each measurement, the working electrodes were manually polished with abrasive paper down to grain P4000. The as-prepared polymer membranes with a mean thickness of 350 μm were cut into circular discs (Ø = 12 mm). The electrochemical stability window was taken as the distance between the electrode potentials where the beginning current rise of the anodic oxidation or cathodic reduction current, respectively, was distinguishable from the capacitive background current.

2.6. Transference number of lithium ions

The lithium transference number t_+ was determined using the steady-state potentiostatic polarization method of Evans, Vincent and Bruce [24]. *Swagelok*®-cells with two symmetric metallic lithium electrodes according to the sequence Li|polymer electrolyte|Li were applied and controlled by a potentiostat (Metrohm PGStat 302 N, Ecochemie together with Nova 1.6 Ecochemie software). The electrode surface areas were $A = 1.13\ cm^2$.

The contribution of the electrode interfaces was determined by AC impedance measurement in the frequency range from 1 Hz to 1 MHz (AC amplitude was ±10 mV). The cell impedance was analyzed before and after each single DC polarization curve $I(t)$. Thin reaction layers often denoted as SEI (=*solid|electrolyte interphase*) formed initially just after assembling the cells as monitored by an initial rapid rise of the cell impedance. The SEI films did not grow further during the polarization experiments. The ohmic part of the metal/polymer interface impedance, namely the resistances $R_{0,b}$ (=homogeneous sample before polarization) and $R_{SS,b}$ (=polarized sample after reaching the steady-state) were determined by analyzing the frequency dependent impedance. They arise from the charge transfer resistance and partially from the ion transport within the SEI layers. The resistance values $R_{0,b}$ and $R_{SS,b}$ were used to eliminate the SEI contribution in the final evaluation from the bulk polarization voltage.

For the potentiostatic polarization, 10 mV was chosen as applied constant DC cell voltage ΔV. After switching-on this DC voltage, the time dependent current $I(t)$ was monitored. The initial current (I_0) and the final steady-state current (I_{SS}) were taken for the calculation of the transference number t_+ according to

$$t_+ = \frac{I_{SS}(\Delta V - I_0 R_{0,b})}{I_0(\Delta V - I_{SS} R_{SS,b})} \tag{2}$$

In order to take into account the change of the polymer electrolyte resistance from $R_{ely,0}$ to $R_{ely,ss}$ during the polarization (due to formation of a concentration gradient), an additional correction according to Abraham et al. [25] was introduced. This correction leads to the following final equation and was used in our experiments:

$$t_+ = \frac{I_{SS} R_{ely,SS}(\Delta V - I_0 R_{0,b})}{I_0 R_{ely,0}(\Delta V - I_{SS} R_{SS,b})} \tag{3}$$

2.7. Conductivity measurements

The total ionic conductivity was determined by impedance spectroscopy in a temperature range from −50 °C to 110 °C. The impedance was measured with an Alpha-1 High Resolution Impedance Analyzer (Novocontrol GmbH). Square pieces of 1 cm^2 were cut out of the polymer electrolyte membranes and put between two stainless steel electrodes. The samples were measured in the frequency range of 20 Hz to 2 MHz for each temperature. The following Eq. (4) was used to calculate the total ionic conductivity of the samples, in which d is the thickness of the polymer electrolyte membrane, R the bulk resistance of the polymer electrolyte (as evaluated from the frequency dependent cell impedance) and A the contact area of the electrodes on the membranes.

$$\sigma(\text{total}) = \frac{d}{R \cdot A} \quad (4)$$

3. Results and discussion

The GPC measurements delivered an average molecular weight of $1.49 \cdot 10^5$ Da, which corresponds to an average of ~400 monomer units (–NPR_2–) along a linear MEEEP molecule (Fig. 1). The polydispersity index was obtained as PDI = 1.32, in agreement with the relatively sharp distribution in Fig. 1, which indicates that no appreciable degradation or chain cleavage occurred during the macromolecular nucleophilic substitution reaction.

Thermal analysis by DSC showed a thermal stability of the pure polymer up to 150 °C and a very low glass transition temperature of $T_g = -79$ °C. The latter gives rise to high flexibility and segmental mobility of the polymer at ambient temperatures. No melting point was found which excludes any partial crystallinity in the samples. Hence, cross-linking was necessary to achieve mechanically stable electrolyte membranes as pure untreated MEEEP is a viscous melt.

Cross-linked MEEEP membranes with different concentrations of LiTFSI and LiBOB were obtained according to Ref. [21] by preparing a solution with the salts and benzophenone (cf. Section 2.2), casting it as a thin layer between Mylar® foils and initiating the cross-linking by UV-irradiation. UV absorption by benzophenone leads to a reactive $n\pi^*$ triplet state which extracts hydrogen from terminal $-OCH_3$ or $-CH_2-$ in the oligoether side chains. The remaining radicals can react further and partially recombine thus leading to cross-linking [25].

The finally obtained cross-linked membranes were mechanically stable, transparent and highly flexible, but strong traction leads to ruptures (see Fig. 2). The thickness of as-prepared polymer electrolyte membranes was around ~350 μm, although this can easily be reduced to much lower values by appropriate pressure. Furthermore, via drop or spin coating, it is easy to produce polymer electrolyte coatings and thin films directly on anodes or cathodes with followed by in-situ cross-linking as described above.

The lithium salt concentration, expressed by the molar ratio O:Li (i.e. O = number of oxygen atoms in the oligoether side chains), was varied from 50:1 up to 24:1 for LiTFSI and from 40:1 up to 24:1 for LiBOB. The dependence of the T_g values on the salt concentration is shown in Table 1 for the cross-linked polymer electrolyte membranes.

As usually observed for polymer electrolytes, an increased salt concentration leads to higher T_g values, as the local coordination between lithium ions and oxygen atoms in the side chains (Scheme 2) lowers the chain mobility. However, cross-linking itself is the most important factor that decreases the mobility in the polymer electrolyte network. Therefore, an optimization has to be found between enough cross-linking for a sufficient mechanical stability and not too much cross-linking in order to leave enough segmental mobility. Anyway, the T_g values around 210 K as obtained here are still low enough which preserves a good molecular mobility between the cross-linking sites in the network and allows a good ion mobility.

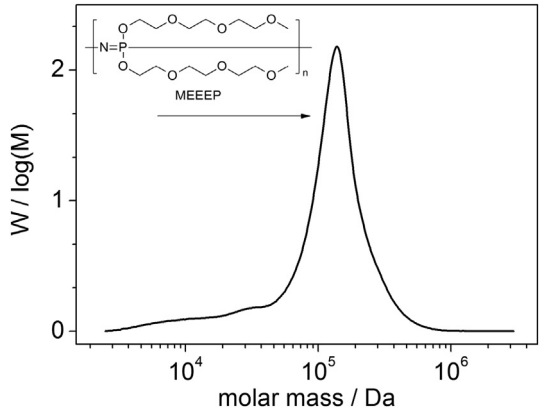

Fig. 1. Molar mass distribution of MEEEP shows long polymer chains with a weight average molecular weight of $<M_N> = 2.2 \cdot 10^5$ g mol^{-1}.

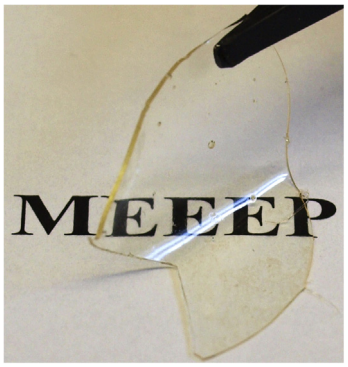

Fig. 2. Typical example of a mechanically stable, transparent and highly flexible MEEEP electrolyte membrane after cross-linking.

The cross-linked membrane samples with a ratio of O:Li = 44:1 for electrolytes with LiTFSI (Fig. 3) and 32:1 for electrolytes with LiBOB (Fig. 4) showed the highest total ionic conductivities at the temperatures of measurement. Two samples with these optimized salt concentrations were additionally analyzed within an enlarged temperature interval between −50 °C and 110 °C. Fig. 5 shows the corresponding temperature dependent conductivities which clearly do not follow an Arrhenius dependence, but a Vogel–Tamman–Fulcher (VTF) behavior, a common observation for most solvent-free polymer electrolytes. Accordingly, in approaching the glass transition temperature, the conductivity decreases towards lower temperatures with a steeply increasing slope [26,27].

The room temperature conductivities of the cross-linked MEEEP membranes in Fig. 5 are $1.2 \cdot 10^{-4}$ S cm^{-1} with LiTFSI and $2.6 \cdot 10^{-5}$ S cm^{-1} with LiBOB. The values are between 1 and 1.5 orders of magnitude higher as compared to our own measurements for dry PEO/LiTFSI electrolyte membranes (with O:Li = 32:1). Similar values for PEO/LiTFSI and PEO/LiBOB electrolytes can be found in the literature [28,29].

Information on the transference number of lithium ions is as important as the total conductivity of a polymer electrolyte itself [30], as the product of the transference number and the total conductivity corresponds to the partial lithium ion conductivity according to

$$\sigma\left(Li^+\right) = t_+ \cdot \sigma(\text{total}) \quad (5)$$

Table 1
Glass transition temperatures of the cross-linked electrolyte membranes containing different amounts of lithium salt.

O:Li	T_g/K (LiTFSI)	T_g/K (LiBOB)
24:1	220	218
32:1	212	212
36:1	–	210
40:1	210	213
44:1	203	–
50:1	203	–

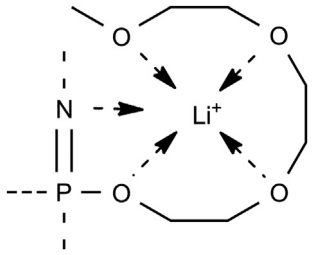

Scheme 2. Possible coordination sites of the lithium cations by the ethylene oxide segments in the side chains. Interaction with the lone pair of the nitrogen atom of the backbone has to be assumed, too [35].

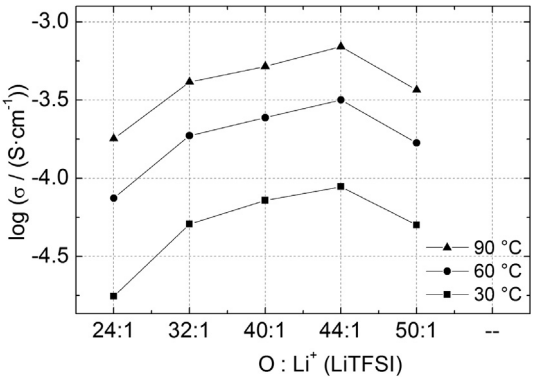

Fig. 3. Ionic conductivities for MEEEP/LiTFSI polymer electrolytes with different salt concentrations in the temperature range 30 °C–90 °C.

The partial lithium ion conductivity (or: effective lithium ion conductivity) is an excellent measure for the steady state lithium ion transport capability of the salt-in MEEEP membranes. This information allows an estimation of the steady state current densities during charging/discharging cycles in corresponding rechargeable lithium polymer cells.

As the lithium transference numbers show similar values for both salts, the lower total ionic conductivity of LiBOB could be addressed to lower anionic mobility in the MEEEP structure and hence a lower dissociation the polymer matrix.

In order to complete the formation of a stable SEI which can be identified by a constant Li metal|polymer interface resistance, all samples had to be held at a constant temperature for 36 h. The final stabilization of the cell interfaces was followed by impedance measurements. As soon as the interface of Li|MEEEP became stable after assembling the cells, the polarization experiment was carried out.

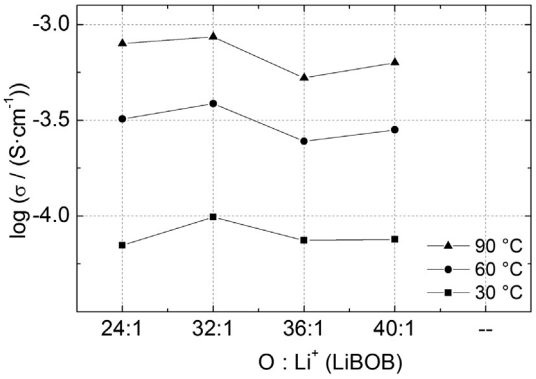

Fig. 4. Ionic conductivities for MEEEP/LiBOB polymer electrolytes with different salt concentrations in the temperature range 30 °C–90 °C.

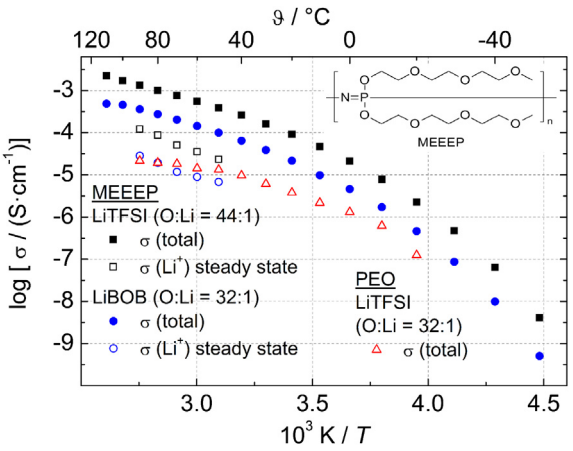

Fig. 5. Temperature dependent conductivity for MEEEP/LiTFSI (O:Li = 44:1) and MEEEP/LiBOB (O:Li = 32:1) and the corresponding effective lithium conductivity during steady state polarization. The ionic conductivity of a corresponding PEO/LiTFSI membrane as measured in the same cell is shown for comparison.

Additional impedance measurements were carried out at the beginning and after the steady state polarization.

The lithium transference number could then be calculated using Eq. (3). The obtained lithium ion transference numbers t_+ are listed in Table 2 for both types of salt-in-MEEEP membranes. The most surprising feature is that lithium transference numbers as low as 0.1 (and less) were obtained which is lower than in other polymer electrolyte systems (typically around 0.2). However, due to the higher total conductivity, the effective lithium ion conductivity calculated according to Eq. (5) for MEEEP/LiTFSI and MEEEP/LiBOB is still equal or even higher for the polyphosphazene based electrolytes as compared to PEO electrolytes with similar concentrations. Fig. 5 shows corresponding values for the partial lithium ion conductivities for our electrolyte membranes as calculated with Eq. (5).

Consequently the partial lithium ion conductivities of MEEEP/LiTFSI or MEEEP/LiBOB are equal or even higher as compared to the total conductivity of PEO/LiTFSI electrolytes at the same temperatures (Fig. 5).

The low lithium ion transference numbers indicate that there is a strong interaction of the lithium ions with the donor atoms of the oligoether grafted polyphosphazene chain. A first explanation may be the steric advantage for formation of coordination complex with lithium ions due to the two oligoether substituents at the phosphorous atoms which can form a local pocket for the cations. A second possibility arises due to the nitrogen atoms along the main chain which are known to bind Lewis acids. Results of ^{15}N NMR and Raman spectroscopy on similar polyphosphazenes support such explanations [28]. An recently published further NMR study revealed an even more detailed overview over the various interaction sites in a typical salt-in-polyphosphazene electrolyte including the 'pocket' effect of the oligoether pairs on the phosphorous [31]. It also delivered further strong support for the non-negligible interaction with the nitrogen atoms of the main chain. Another recent study inferred a predominant contribution of

Table 2
Experimentally determined lithium ion transference numbers t_+ for salt concentrations corresponding to O:LiTFSI = 44:1 and O:LiBOB = 32:1 in MEEEP membranes from 50 °C to 90 °C.

MEEEP	50 °C	60 °C	70 °C	80 °C	90 °C
+LiTFSI	0.060	0.064	0.067	0.087	0.092
+LiBOB	0.068	0.062	0.058	0.070	0.079

anions to charge transport as well from conductivity measurements on salt-in-polymer electrolytes based on the closely related polyphosphazene MEEEP [32] which also confirms our results for the transference numbers.

As Fig. 5 shows, the salt-in-MEEEP membranes deliver high total ionic conductivities at elevated temperatures of ~100 °C with no indication for degradation. Such electrolyte membranes allow higher operation temperatures in corresponding lithium ion cells as compared to cells with conventional standard electrolytes which start to degrade at temperatures above 65 °C.

Figs. 6 and 7 show cyclic voltammograms at 70 °C used to determine the electrochemical stability of our cross-linked polymer electrolyte membranes. As can be expected due to the close analogy regarding the polyether content, the two MEEEP membranes show quite similar anodic oxidation stability limits as compared to PEO based membranes, for which anodic stability limits up to 4.5 V were reported in the literature as well [33–36]. The voltammograms also correlate well with those of Abraham et al. [37] for closely related polyphosphazene based electrolytes.

The anodic oxidation scan of the CV curves show a beginning increase of the current density above 4.4 V for MEEEP/LiTFSI and above 4.7 V for MEEEP/LiBOB. In both the cases, the anodic oxidation at these electrode potentials is attributed to irreversible oxidation steps in the oligoether side chains of the polymer [1]. Under oxygen free conditions and in the absence of parallel oxidation of the salt anions, these correspond most probably to radical reactions initiated by anodic hydrogen abstraction leaving carbon radicals on the polyether chains and followed by recombination and further radical reactions among the polymer molecules.

The cathodic reduction scans at low electrode potentials, as expected, show the reversible lithium deposition and dissolution around 0 V. The current densities for lithium deposition are limited by the resistance of the SEI. For the membranes with LiBOB, the cathodic current densities for lithium deposition are smaller than those observed for the LiTFSI containing membranes. This is partially due to the lower total conductivity and partially due to the higher resistance of the SEI of the LiBOB containing electrolyte membranes. The latter is a desired effect which helps to suppress the problematic cathodic lithium dendrite growth at the lithium metal surface and to achieve reversible cycling at lithium metal electrodes. The reversible peaks in the anodic range at ~0.4 V and 0.8 V, which can be found for both cyclic voltammograms, are assigned to a lithium plating/stripping process on the nickel electrode [38]. The small irreversible increase in the current density at ~1.7 V for the MEEEP/LiBOB membrane is caused by a LiBOB reduction and hence shows SEI formation.

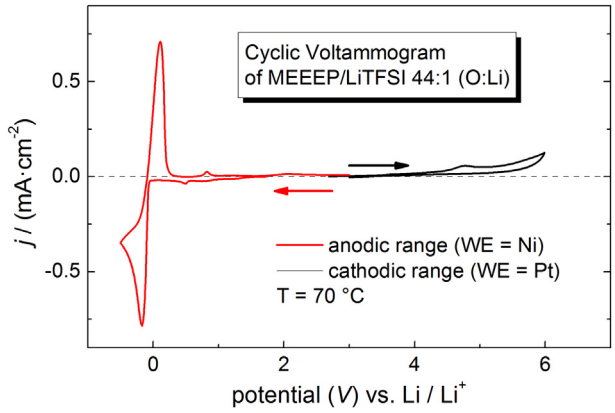

Fig. 6. Cyclic voltammogram of MEEEP with a salt concentration corresponding to O:LiTFSI = 44:1 at 70 °C. WE (=working electrode): Ni and Pt.

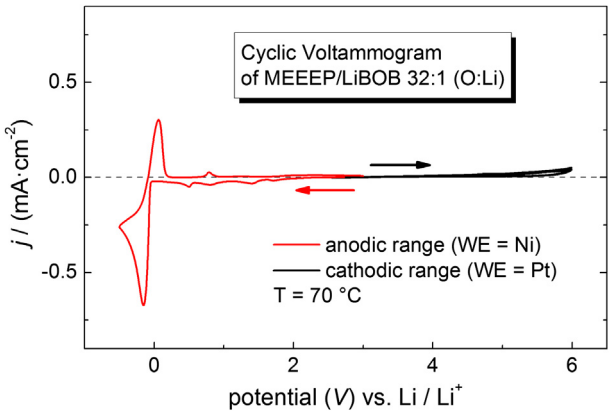

Fig. 7. Cyclic voltammogram of MEEEP with a salt concentration corresponding to O:LiBOB = 32:1 at 70 °C. WE (=working electrode): Ni and Pt.

Apart from that, it is remarkable that no degradation reactions were observed of the MEEEP polymer during the long time measurements at low electrode potentials in contact to lithium metal electrodes. Hence, the oligoether grafted polyphosphazene based electrolytes are promising candidates for testing with high energy density lithium cells using lithium metal anodes.

4. Conclusions

All cross-linked MEEEP polymer electrolytes formed amorphous salt-in-polymer solutions with similar characteristics like low glass transition temperatures and higher dimensional stability compared to not cross-linked systems. The observed electrochemical stability allows the use of oligoether grafted polyphosphazenes at high cell voltages up to 4.7 V against Li/Li$^+$, as well as in the presence of lithium metal anodes due to formation of a stable SEI.

The only drawback of polyphosphazene based electrolytes is the low lithium transference number. However, taking into account the lower total conductivity of electrolytes with PEO as compared to those of corresponding polyphosphazenes, the effective lithium ion conductivity (=product of total conductivity and lithium ion transference number) is still higher for the polyphosphazene electrolytes. For PEO based electrolytes, improvements of lithium transference were reported by applying chemical additives or particle dispersions in this context. Hence, it is very probable to achieve improvements for the lithium transference numbers of polyphosphazene electrolytes in the same way as for PEO electrolytes. First tests already showed promising results for polymeric gels based on polyphosphazenes.

Overall, the high thermal and electrochemical stability and the good experiences with a stable SEI protected interface at lithium metal electrodes make MEEEP interesting for lithium battery cells with lithium metal anodes.

Acknowledgments

The funding by the Deutsche Forschungsgemeinschaft within the grant “Functional Materials and Materials Analysis for Lithium-High-Performance Batteries” (PAK 177-Wi 952-2) is gratefully acknowledged. Furthermore, the authors thank R. Stolina and T. Schürmann for useful hints and discussion.

References

[1] K. Xu, Chem. Rev. 104 (2004) 4303–4417.
[2] F. Gray, M. Armand, in: J.O. Besenhard (Ed.), Handbook of Battery Materials, Wiley-VCH, Weinheim; New York, 1999, pp. 499–523.

[3] D.E. Fenton, J.M. Parker, P.V. Wright, Polymer 14 (1973) 589.
[4] M. Armand, J.M. Chabagno, M.J. Duclot, in: Extended Abstracts: Second International Meeting on Solid Electrolytes, 1978.
[5] M. Armand, Solid State Ionics 9–10 (Part 2) (1983) 745–754.
[6] W.H. Meyer, Adv. Mater. 10 (1998) 439.
[7] M.A. Ratner, D.F. Shriver, Chem. Rev. 88 (1988) 109–124.
[8] P.M. Blonsky, D.F. Shriver, P. Austin, H.R. Allcock, J. Am. Chem. Soc. 106 (1984) 6854–6855.
[9] P.M. Blonsky, D.F. Shriver, P. Austin, H.R. Allcock, Solid State Ionics 18–19 (1986) 258–264.
[10] N. Kaskhedikar, J. Paulsdorf, M. Burjanadze, Y. Karatas, D. Wilmer, B. Roling, H.-D. Wiemhöfer, Solid State Ionics 177 (2006) 703–707.
[11] J. Paulsdorf, M. Burjanadze, K. Hagelschur, H.-D. Wiemhöfer, Solid State Ionics 169 (2004) 25–33.
[12] H.R. Allcock, S.E. Kuharcik, C.S. Reed, M.E. Napierala, Macromolecules 29 (1996) 3384–3389.
[13] H.R. Allcock, S.J.M. Oconnor, D.L. Olmeijer, M.E. Napierala, C.G. Cameron, Macromolecules 29 (1996) 7544–7552.
[14] H.R. Allcock, P.E. Austin, T.X. Neenan, J.T. Sisko, P.M. Blonsky, D.F. Shriver, Macromolecules 19 (1986) 1508–1512.
[15] H.R. Allcock, Soft Matter 8 (2012) 7521–7532.
[16] B. Wang, Macromolecules 38 (2005) 643–645.
[17] J. Paulsdorf, N. Kaskhedikar, M. Burjanadze, S. Obeidi, N.A. Stolwijk, D. Wilmer, H.D. Wiemhöfer, Chem. Mater. 18 (2006) 1281–1288.
[18] A. Fedorková, R. Oriňáková, A. Oriňák, I. Talian, A. Heile, H.-D. Wiemhöfer, D. Kaniansky, H.F. Arlinghaus, J. Power Sources 195 (2010) 3907–3912.
[19] Y.-H. Huang, K.-S. Park, J.B. Goodenough, J. Electrochem. Soc. 153 (2006) A2282–A2286.
[20] G.X. Wang, L. Yang, Y. Chen, J.Z. Wang, S. Bewlay, H.K. Liu, Electrochim. Acta 50 (2005) 4649–4654.
[21] B. Wang, E. Rivard, I. Manners, Inorg. Chem. 41 (2002) 1690.
[22] H.R. Allcock, S.D. Reeves, C.R. de Denus, C.A. Crane, Macromolecules 34 (2001) 748–754.
[23] C.J. Nelson, W.D. Coggio, H.R. Allcock, Chem. Mater. 3 (1991) 786–787.
[24] P.G. Bruce, J. Evans, C.A. Vincent, Solid State Ionics 28–30 (Part 2) (1988) 918–922.
[25] K.M. Abraham, Z. Jiang, B. Carroll, Chem. Mater. 9 (1997) 1978–1988.
[26] N.A. Stolwijk, J. Kösters, M. Wiencierz, M. Schönhoff, Electrochim. Acta 102 (2013) 451–458.
[27] N.A. Stolwijk, M. Wiencierz, S. Obeidi, Electrochim. Acta 53 (2007) 1575–1583.
[28] P.A.R.D. Jayathilaka, M.A.K.L. Dissanayake, I. Albinsson, B.E. Mellander, Electrochim. Acta 47 (2002) 3257–3268.
[29] H.H. Sumathipala, J. Hassoun, S. Panero, B. Scrosati, Ionics 13 (2007) 281–286.
[30] M. Doyle, T.F. Fuller, J. Newman, Electrochim. Acta 39 (1994) 2073–2081.
[31] L. van Wüllen, T.K.J. Köster, H.-D. Wiemhöfer, N. Kaskhedikar, Chem. Mater. 20 (2008) 7399–7407.
[32] D.K. Lee, H.R. Allcock, Solid State Ionics 181 (2010) 1721–1726.
[33] Y. Kang, J. Lee, J.-i. Lee, C. Lee, J. Power Sources 165 (2007) 92–96.
[34] B. Oh, D. Vissers, Z. Zhang, R. West, H. Tsukamoto, K. Amine, J. Power Sources 119–121 (2003) 442–447.
[35] C.H. Park, D.W. Kim, J. Prakash, Y.-K. Sun, Solid State Ionics 159 (2003) 111–119.
[36] F.-M. Wang, C.-C. Hu, S.-C. Lo, Y.-Y. Wang, C.-C. Wan, Solid State Ionics 180 (2009) 405–411.
[37] K.M. Abraham, M. Alamgir, Chem. Mater. 3 (1991) 339–348.
[38] L.-F. Li, D. Totir, Y. Gofer, G.S. Chottiner, D.A. Anderson, Electrochim. Acta 44 (1998) 949.